

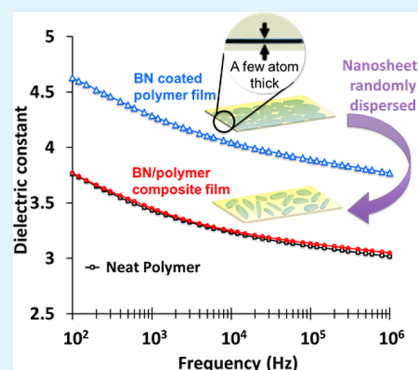
## Boron Nitride Surface Activity as Route to Composite Dielectric Films

Zhenhua Cui,<sup>†</sup> Zhen Cao,<sup>†</sup> Rui Ma,<sup>†</sup> Andrey V. Dobrynin,<sup>\*,§</sup> and Douglas H. Adamson<sup>\*,†,‡</sup><sup>†</sup>Polymer Program, Institute of Materials Science, and <sup>‡</sup>Department of Chemistry, University of Connecticut, Storrs, Connecticut 06269, United States<sup>§</sup>Department of Polymer Science, University of Akron, Akron, Ohio 44325, United States

## Supporting Information

**ABSTRACT:** The propensity of boron nitride sheets to stack creates obstacles for their application as multifunctional materials despite their unique thermal, mechanical, and electrical properties. To address this challenge, we use a combination of molecular dynamics simulations and experimental techniques to demonstrate surfactant-like properties of BN sheets at the interface between immiscible solvents. The spreading of two-dimensional BN sheets at a high-energy oil/water interface lowers the free energy of the system, creating films of overlapping BN sheets that are more thermodynamically favorable than stacked sheets. Coating such films onto polymers results in composite materials with exceptional barrier and dielectric properties.

**KEYWORDS:** boron nitride, dielectrics, polymeric films, interface trapping, exfoliation, molecular dynamics simulations, coating, composites



The exceptional thermal, mechanical, and electrical properties of high-aspect-ratio hexagonal boron nitride (BN) sheets make BN an attractive candidate for the design of multifunctional composite materials. However, similar to graphene, BN's propensity to restack after exfoliation, coupled with its chemical inertness, creates obstacles for its applications.<sup>1–3</sup> Although graphite, composed of only carbon, is known to be an electrical conductor, the different electronegativities of boron and nitrogen result in BN being an insulator with a large bandgap (ca. 6 eV),<sup>4,5</sup> a dielectric constant of about 5,<sup>6</sup> and a breakdown voltage of 800 MV/m,<sup>7,8</sup> suggesting a tremendous potential for electronic and energy storage applications.<sup>6,9–20</sup>

Rather than meeting the challenge of BN exfoliation and stabilization by chemical functionalization, as is commonly done with graphite, in this paper, we outline a thermodynamically driven approach for the exfoliation and stabilization of BN at the interface between immiscible solvents. We provide computational and experimental verification that the spreading of two-dimensional BN sheets at a high-energy oil/water interface lowers the free energy of the system, creating a situation in which films of overlapping BN sheets are more thermodynamically stable than stacked sheets. Thus, by rearranging the BN sheets from a stacked morphology to an overlapping arrangement of BN sheets covering an interface, the system lowers its energy. This interfacial exfoliation technique allows for the creation of BN films only a few sheets thick. The simplicity of this approach provides a significant advantage over CVD grown BN films that are brittle, hard to transfer, and expensive to produce.<sup>14,18,19,21</sup> When the spread-

ing technique is applied to coat polymer films with thin layers of overlapping BN sheets, the composite films have exceptional barrier and dielectric properties with a low frequency dielectric constant approaching 5, and reliable energy storage capacity estimated to be  $\sim 4.9$  J/cm<sup>3</sup> for PMMA/BN composite films.

To demonstrate the BN sheet's surfactant-like properties and to understand the mechanism of the BN sheet's interface localization, we perform all atom molecular dynamics simulations of BN sheets at the interface between water and heptane. In these simulations, we use the TIP3P force field potential for water and the Generalized Amber Force Field for the atomistic model of heptane. The boron nitride sheets are modeled as polycyclic boron nitride consisting of eight generations (G8) of BN rings terminated by hydrogen, B<sub>192</sub>N<sub>192</sub>H<sub>48</sub>. The partial charges on the heptane and the G8 BN sheets are obtained from the Mulliken population analysis from ab initio calculations using the Gaussian 09 simulation package with the 6-31G(d) basis set and B3LYP DFT (see the Supporting Information). The parameters for potentials describing deformations of the bonds, bond angles, dihedral angles and improper angles are obtained by performing DFT calculations of the in-plane and out-of-plane G8 BN sheet deformations as described in the Supporting Information. In our molecular dynamics simulations we study water/heptane systems containing one, four and nine BN sheets, with the number of water and heptane molecules given in Table S1. All

Received: June 11, 2015

Accepted: July 27, 2015

Published: July 27, 2015

simulations are performed at  $T = 300$  K and pressure equal to 1 atm. The simulations are performed following methodology developed for modeling graphene flakes in water/heptane mixtures.<sup>23</sup> The details of the simulation procedure are described in the [Supporting Information](#).

**Figure 1A** shows the distribution function of the atoms belonging to water, heptane and BN sheets obtained from

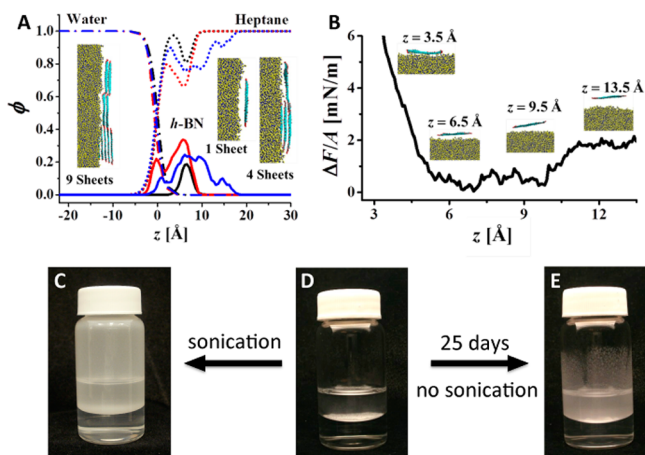


**Figure 1.** (A) Number fraction distributions of atoms belonging to water molecules, heptane molecules, and BN sheets along the  $z$ -axis normal to the water/heptane interface for water/heptane mixtures containing a single BN sheet (black lines), four BN sheets (red lines), and nine BN sheets (blue lines). Number fraction distribution curves of atoms belonging to water molecules, heptane molecules and BN sheets are shown as dash-dot lines, dot lines, and solid lines, respectively. The location of the origin of the  $z$ -axis is set to the point where the number fraction of atoms belonging to water molecules outside the region occupied by the BN sheets decreases by half from its bulk value of  $\phi_{\text{wat}} = 0.5$ . Insets show typical configurations of the BN layers at the water/heptane interface. Solvent shown is water, and heptane molecules are transparent. (B) Variation in the potential of the mean force normalized by the BN sheet surface area along the  $z$ -axis normal to the water/heptane interface. Insets show typical sheet configurations. The heptane phase is transparent. (C) Heptane/water mixture with BN following brief bath sonication. (D) Water/heptane/BN initial sample. (E) Water/heptane/BN sample after sitting for 25 days with no sonication.

molecular dynamics simulations of the systems containing a single sheet, four sheets, and nine sheets of BN. For multisheet simulations we observe the aggregation of the BN sheets and formation of a BN skin at the interface between water and heptane (see insets in [Figure 1A](#)). Formation of the multisheet aggregates is indicated by the appearance of the multiple peaks in the distribution function seen in [Figure 1A](#). It is interesting to note that the single BN sheet resides close to the water/heptane interface, but in the heptane phase, whereas sheets belonging to multisheet aggregates can penetrate into the water phase in order to allow accommodation of the assembly in the interface region.

To establish the affinity of BN sheets to the water/heptane interface, we calculate the potential of the mean force along the  $z$ -axis normal to the water/heptane interface (see [Figure 1B](#)) by using the Weighted Histogram Analysis Method. The minimum of the potential is located in the heptane phase, indicating the preference of BN for heptane rather than water. The increase of the potential in the heptane phase is not as steep as that observed in the water phase, an indication that heptane is a

better solvent for BN than is water. The magnitude of the potential in the plateau regime is on the order of 1.8 mN/m. This free energy change is lower than the corresponding 2.2 mN/m change of the free energy obtained for graphene displacement from an interface using similar calculations.<sup>23,24</sup> Using this value, we estimate the work required to displace BN sheets with  $100 \times 100$  nm lateral dimensions from the water/heptane interface into the heptane phase to be  $4420 k_B T$ . This energy is sufficiently strong to localize the BN sheet at the water/heptane interface.

Results of our molecular dynamics simulations indicate that localization and spreading of BN sheets at the interface is driven by a reduction in the interfacial energy between oil and water. In order to experimentally confirm that this rearrangement of BN sheets results in a new thermodynamic minimum for the system, we study the exfoliation and spreading of boron nitride at a water/heptane interface. When BN powder is placed in a clean glass vial, the BN is observed to reside at the heptane/water interface. After low power bath sonication for 30 s, the BN spreads at the interface and also climbs the wall of the vial as it stabilizes the interface between the layer of water on the hydrophilic glass and the heptane vapor as shown in [Figure 1C](#). More importantly, the BN is also observed to spread and climb the glass vial wall without the use of sonication, although at a significantly slower rate. This is illustrated in [Figure 1E](#), and the initial mixture is shown in [Figure 1D](#). This behavior is analogous to that observed for graphite in previous studies.<sup>23,24</sup>

Because the BN sheets spread at the water wet hydrophilic glass surfaces of a vial that are in contact with an oil phase, they also climb the surface of glass slides placed in a vial. [Figure 2A](#)

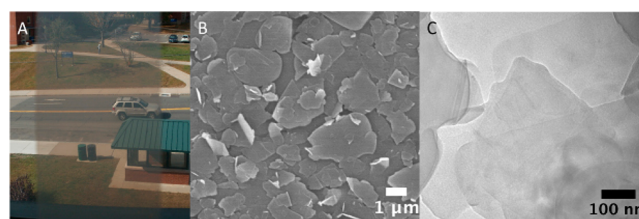
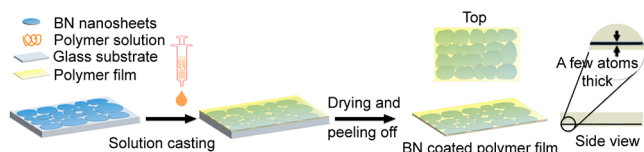


**Figure 2.** Images of boron nitride films. (A) Picture of film on a glass microscope slide. (B) SEM image of film showing individual sheets. (C) TEM image of film demonstrating the film to be composed of overlapping sheets.

shows such a glass slide covered with a BN film. These films consist of overlapping sheets of BN as illustrated by the SEM image shown in [Figure 2B](#), where the sheets comprising the film are clearly visible and have lateral dimensions of several microns. The degree of TEM contrast in [Figure 2C](#) suggests that the film consists of overlapping BN sheets. Regions with no sheets, one sheet, and two to three sheets are apparent, with approximately 10% of the surface containing no sheets. A lower magnification image is included in the [Supporting Information](#) to help illustrate the overlapping nature of the sheets comprising the film. The presence of single-layer BN sheets in the film is also confirmed by the peak at  $1369 \text{ cm}^{-1}$  in the Raman spectra shown in the [Supporting Information](#).<sup>22</sup> Additionally, electron diffraction patterns reveal the typical 6-fold symmetry structure of BN sheets, also shown in the [Supporting Information](#).

The overlapping BN sheets on the glass slide are transferred to a polymer surface by drop casting a polymer solution onto the dried BN film. This procedure is presented in [Scheme 1. A](#)

### Scheme 1. Illustration of Preparation of Polymer Film Coated with Overlapping BN Sheets



solution of PMMA in tetrahydrofuran (THF) is placed on the BN film and allowed to dry. Figure 3A shows a BN film covered

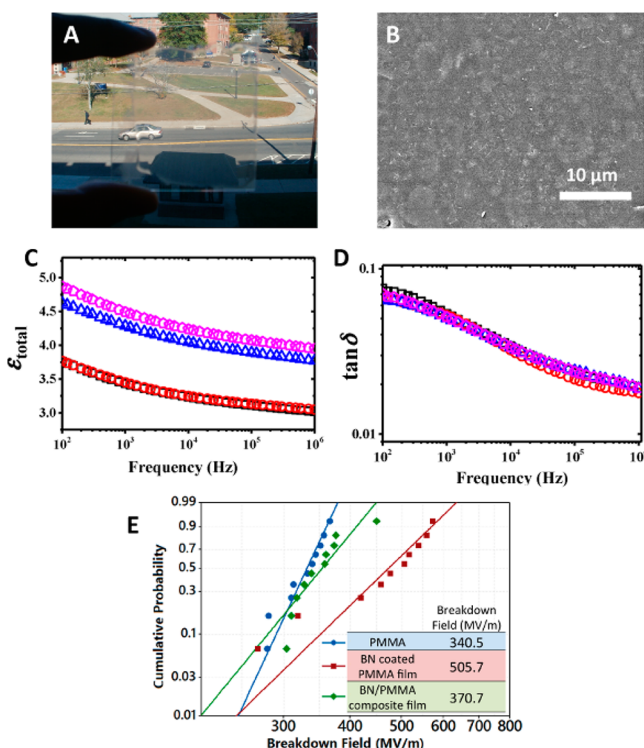


**Figure 3.** (A) Photograph of PMMA film coated with BN. (B) SEM image of BN coating on PMMA film, showing the BN sheets imbedded in the polymer. (C) Dielectric constant at room temperature as a function of frequency for unmodified PMMA film (black squares, lower curve), BN-PMMA film with dispersed BN sheets (red circles overlapping black squares), and BN-coated PMMA film with thickness 78.8  $\mu\text{m}$  (blue triangles), 44.5  $\mu\text{m}$  (pink pentagons). (D) The loss ratio as a function of frequency (curves have the same identity as in C). (E) Breakdown voltage of BN coated PMMA as determined with the Wiebull distribution.

with a layer of PMMA before it is peeled off the slide. The BN film is embedded on the surface of the polymer as illustrated by the SEM image in Figure 3B, where the outline of flat BN sheets covered by polymer can be clearly seen. To confirm that a thin layer of polymer resides on top of the BN sheets, the electron beam of the SEM is focused on a small area as shown in Figure S7. After exposure for less than a minute, the covering polymer layer degrades, revealing the embedded BN sheets just below the surface.

To investigate the role played by the overlapping BN sheet morphology, as opposed to a possible bulk effect of BN, a control polymer film is prepared containing a mass of BN equal that found in the BN film, but without the continuous film morphology. To do this, a PMMA film with a BN coating is dissolved in THF, and then recast onto a glass slide followed by

THF evaporation. This procedure removes the exfoliated BN film morphology and makes a PMMA film with BN sheets randomly dispersed, and possibly restacked, within it. The properties of the three samples are then compared: the BN-coated polymer films, neat PMMA films, and PMMA films containing BN but lacking the overlapping sheet morphology.

The PMMA-coated with a BN film shows a significant increase in dielectric constant as compared to both the neat PMMA films and the PMMA films filled with randomly mixed BN sheets (see Figure 3C). Additionally, the loss ratio of coated PMMA is not affected by the BN sheets, as might be expected for such a low loading (less than 0.01% by mass) (Figure 3D). The significant improvement of the dielectric properties of the thin layer BN coated polymer film is attributed to the presence of the continuous overlapping BN sheets that constitute the thin BN layer. We observe that the dielectric properties of the thinner polymer films are better in comparison with thicker samples. For thinner samples, the contribution of the BN layer to the total film's dielectric properties is proportionally greater. Note that this change in film dielectric properties is consistent with a recent study of a BN/graphene nanocapacitor in which a significant increase (from 4.9 to as high as 12) of the dielectric constant of BN sheets was observed as the number of layers decreased from 16 to 2.<sup>6</sup> We also observe, in addition to improvements in the dielectric constant, that the breakdown field of the few-layer BN coated PMMA film increases by approximately 50% from 340.5 MV/m for pure PMMA to 505.7 MV/m, as determined using a linear voltage ramp and the Weibull distribution, as shown in Figure 3E. Using the value of the dielectric constant at 1 kHz and the breakdown field, we calculate the energy density,  $\epsilon\epsilon_0 E^2/2$  (where  $\epsilon_0 = 8.85 \times 10^{-12}$  F/m is the dielectric permittivity of the vacuum), for BN-coated PMMA film to be 4.85 J/cm<sup>3</sup>. Thus, the presence of the BN layer has the potential to increase the stored energy density by 2.76 times in comparison with that for pure PMMA. Note that this value of the stored energy is greater than that for the state-of-the-art biaxially oriented polypropylene film capacitor.<sup>25</sup>

The BN film coating, in addition to improving the electrical properties of the polymer film, also improves the polymer's barrier properties. Without the BN coating, PMMA obtaining by drop casting from a THF solution allows the permeation of gas at the rate of  $2.347 \times 10^{-14}$  cm<sup>3</sup> cm/cm<sup>2</sup> s Pa. The presence of the BN layer, even though less than four sheets thick and with approximately 10% uncovered area, results in decrease of the gas permeation to  $2.845 \times 10^{-14}$  cm<sup>3</sup> cm/cm<sup>2</sup> s Pa. This is nearly a 21% change with a loading of less than 0.01%. The presence of a near continuous coating of the polymer with overlapping BN sheets seems the only plausible explanation for such a large effect from such a small loading.

In this paper, we demonstrate the surface activity of BN sheets for water/oil interfaces and utilize the spreading driven by this surface activity for the preparation of films consisting of few-layer overlapping BN sheets. Using molecular dynamics simulations, we explain the mechanism of BN sheet spreading and show that this spreading is driven by the minimization of the system free energy. BN films produced by the sheets' spreading are coated onto polymer films, resulting in significant alterations in the properties of the films at extremely low loadings of the overlapping BN sheets. These property changes include increases in dielectric constant and breakdown electric field, and decreases in gas permeation. The inexpensive and straightforward formation and application of these BN-based

composite films, coupled with their significant property enhancements, make them a promising material, with a low barrier of entry, for applications in electronics and energy storage.

## ■ ASSOCIATED CONTENT

### Supporting Information

The Supporting Information is available free of charge on the ACS Publications website at DOI: 10.1021/acsami.5b05092.

experimental procedures, details of BN thin films and BN-coated polymer sample preparation, films characterizations, and details of the computational study (PDF)

## ■ AUTHOR INFORMATION

### Corresponding Authors

\*E-mail: adamson@uconn.edu.

\*E-mail: adobrynin@uakron.edu.

### Notes

The authors declare no competing financial interest.

## ■ ACKNOWLEDGMENTS

Computer simulations for this work was performed at the U.S. Department of Energy, Center for Integrated Nanotechnologies, at Los Alamos National Laboratory (Contract DE-AC52-06NA25396) and Sandia National Laboratories. Sandia is a multiprogram laboratory operated by Sandia Corporation, a Lockheed Martin Company, for the United States Department of Energy under Contract DE-AC04-94AL85000. Funding from the UConn Development Fund is also gratefully acknowledged.

## ■ REFERENCES

- (1) Coleman, J. N.; Lotya, M.; O'Neill, A.; Bergin, S. D.; King, P. J.; Khan, U.; Young, K.; Gaucher, A.; De, S.; Smith, R. J.; Shvets, I. V.; Arora, S. K.; Stanton, G.; Kim, H.-Y.; Lee, K.; Kim, G. T.; Duesberg, G. S.; Hallam, T.; Boland, J. J.; Wang, J. J.; Donegan, J. F.; Grunlan, J. C.; Moriarty, G.; Shmeliov, A.; Nicholls, R. J.; Perkins, J. M.; Grievson, E. M.; Theuwissen, K.; McComb, D. W.; Nellist, P. D.; Nicolosi, V. Two-Dimensional Nanosheets Produced by Liquid Exfoliation of Layered Materials. *Science* **2011**, *331* (6017), 568–571.
- (2) Wang, X.; Zhi, C.; Li, L.; Zeng, H.; Li, C.; Mitome, M.; Golberg, D.; Bando, Y. "Chemical Blowing" of Thin-Walled Bubbles: High-Throughput Fabrication of Large-Area, Few-Layered BN and Cx-BN Nanosheets. *Adv. Mater.* **2011**, *23* (35), 4072–4076.
- (3) Pierret, A.; Loayza, J.; Berini, B.; Betz, A.; Plaçais, B.; Ducastelle, F.; Barjon, J.; Loiseau, A. Excitonic Recombinations in h-BN: From Bulk to Exfoliated Layers. *Phys. Rev. B* **2014**, *89* (3), 035414.
- (4) Watanabe, K.; Taniguchi, T.; Kanda, H. Direct-Bandgap Properties and Evidence for Ultraviolet Lasing of Hexagonal Boron Nitride Single Crystal. *Nat. Mater.* **2004**, *3* (6), 404–409.
- (5) Zunger, A.; Katzir, A.; Halperin, A. Optical Properties of Hexagonal Boron Nitride. *Phys. Rev. B* **1976**, *13* (12), 5560–5573.
- (6) Shi, G.; Hanlumyuang, Y.; Liu, Z.; Gong, Y.; Gao, W.; Li, B.; Kono, J.; Lou, J.; Vajtai, R.; Sharma, P.; Ajayan, P. M. Boron Nitride-Graphene Nanocapacitor and the Origins of Anomalous Size-Dependent Increase of Capacitance. *Nano Lett.* **2014**, *14* (4), 1739–1744.
- (7) Young, A. F.; Dean, C. R.; Meric, I.; Sorgenfrei, S.; Ren, H.; Watanabe, K.; Taniguchi, T.; Hone, J.; Shepard, K. L.; Kim, P. Electronic Compressibility of Layer-Polarized Bilayer Graphene. *Phys. Rev. B: Condens. Matter Mater. Phys.* **2012**, *85* (23), 235458.
- (8) Dean, C. R.; Young, A. F.; Meric, I.; Lee, C.; Wang, L.; Sorgenfrei, S.; Watanabe, K.; Taniguchi, T.; Kim, P.; Shepard, K. L.; Hone, J. Boron nitride substrates for high-quality graphene electronics. *Nat. Nanotechnol.* **2010**, *5* (10), 722–726.
- (9) Kim, K. K.; Hsu, A.; Jia, X.; Kim, S. M.; Shi, Y.; Dresselhaus, M.; Palacios, T.; Kong, J. Synthesis and Characterization of Hexagonal Boron Nitride Film as a Dielectric Layer for Graphene Devices. *ACS Nano* **2012**, *6* (10), 8583–8590.
- (10) Li, Q.; Han, K.; Gadinski, M. R.; Zhang, G.; Wang, Q. High Energy and Power Density Capacitors from Solution-Processed Ternary Ferroelectric Polymer Nanocomposites. *Adv. Mater.* **2014**, *26* (36), 6244–6249.
- (11) Takahashi, S.; Imai, Y.; Kan, A.; Hotta, Y.; Ogawa, H. Dielectric and Thermal Properties of Isotactic Polypropylene/Hexagonal Boron Nitride Composites for High-Frequency Applications. *J. Alloys Compd.* **2014**, *615*, 141–145.
- (12) Wang, X.; Pakdel, A.; Zhang, J.; Weng, Q.; Zhai, T.; Zhi, C.; Golberg, D.; Bando, Y. Large-Surface-Area BN Nanosheets and their Utilization in Polymeric Composites with Improved Thermal and Dielectric Properties. *Nanoscale Res. Lett.* **2012**, *7* (1), 1–7.
- (13) Zhang, C.; Fu, L.; Zhao, S.; Zhou, Y.; Peng, H.; Liu, Z. Controllable Co-segregation Synthesis of Wafer-Scale Hexagonal Boron Nitride Thin Films. *Adv. Mater.* **2014**, *26* (11), 1776–1781.
- (14) Liu, Z.; Song, L.; Zhao, S.; Huang, J.; Ma, L.; Zhang, J.; Lou, J.; Ajayan, P. M. Direct Growth of Graphene/Hexagonal Boron Nitride Stacked Layers. *Nano Lett.* **2011**, *11* (5), 2032–2037.
- (15) Osada, M.; Sasaki, T. Two-Dimensional Dielectric Nanosheets: Novel Nanoelectronics from Nanocrystal Building Blocks. *Adv. Mater.* **2012**, *24* (2), 210–228.
- (16) Britnell, L.; Gorbachev, R. V.; Jalil, R.; Belle, B. D.; Schedin, F.; Mishchenko, A.; Georgiou, T.; Katsnelson, M. I.; Eaves, L.; Morozov, S. V.; Peres, N. M. R.; Leist, J.; Geim, A. K.; Novoselov, K. S.; Ponomarenko, L. A. Field-Effect Tunneling Transistor Based on Vertical Graphene Heterostructures. *Science* **2012**, *335* (6071), 947–950.
- (17) Lee, K. H.; Shin, H.-J.; Lee, J.; Lee, I.-y.; Kim, G.-H.; Choi, J.-Y.; Kim, S.-W. Large-Scale Synthesis of High-Quality Hexagonal Boron Nitride Nanosheets for Large-Area Graphene Electronics. *Nano Lett.* **2012**, *12* (2), 714–718.
- (18) Wang, L.; Wu, B.; Chen, J.; Liu, H.; Hu, P.; Liu, Y. Monolayer Hexagonal Boron Nitride Films with Large Domain Size and Clean Interface for Enhancing the Mobility of Graphene-Based Field-Effect Transistors. *Adv. Mater.* **2014**, *26* (10), 1559–1564.
- (19) Wang, M.; Jang, S. K.; Jang, W.-J.; Kim, M.; Park, S.-Y.; Kim, S.-W.; Kahng, S.-J.; Choi, J.-Y.; Ruoff, R. S.; Song, Y. J.; Lee, S. A Platform for Large-Scale Graphene Electronics-CVD Growth of Single-Layer Graphene on CVD-Grown Hexagonal Boron Nitride. *Adv. Mater.* **2013**, *25* (19), 2746–2752.
- (20) Zhang, G.; Li, Q.; Gu, H.; Jiang, S.; Han, K.; Gadinski, M. R.; Haque, M. A.; Zhang, Q.; Wang, Q. Ferroelectric Polymer Nanocomposites for Room-Temperature Electrocaloric Refrigeration. *Adv. Mater.* **2015**, *27* (8), 1450–1454.
- (21) Song, L.; Ci, L.; Lu, H.; Sorokin, P. B.; Jin, C.; Ni, J.; Kvashnin, A. G.; Kvashnin, D. G.; Lou, J.; Yakobson, B. I.; Ajayan, P. M. Large Scale Growth and Characterization of Atomic Hexagonal Boron Nitride Layers. *Nano Lett.* **2010**, *10* (8), 3209–3215.
- (22) Gorbachev, R. V.; Riaz, I.; Nair, R. R.; Jalil, R.; Britnell, L.; Belle, B. D.; Hill, E. W.; Novoselov, K. S.; Watanabe, K.; Taniguchi, T.; Geim, A. K.; Blake, P. Hunting for Monolayer Boron Nitride: Optical and Raman Signatures. *Small* **2011**, *7* (4), 465–468.
- (23) Woltornist, S. J.; Oyer, A. J.; Carrillo, J.-M. Y.; Dobrynin, A. V.; Adamson, D. H. Conductive Thin Films of Pristine Graphene by Solvent Interface Trapping. *ACS Nano* **2013**, *7* (8), 7062–7066.
- (24) Woltornist, S. J.; Carrillo, J.-M. Y.; Xu, T. O.; Dobrynin, A. V.; Adamson, D. H. Polymer/Pristine Graphene Based Composites: From Emulsions to Strong, Electrically Conductive Foams. *Macromolecules* **2015**, *48* (3), 687–693.
- (25) Chu, B.; Zhou, X.; Ren, K.; Neese, B.; Lin, M.; Wang, Q.; Bauer, F.; Zhang, Q. M. A Dielectric Polymer with High Electric Energy Density and Fast Discharge Speed. *Science* **2006**, *313* (5785), 334–336.